

This is a repository copy of  *$\beta$ -delayed fission of  $^{192,194}\text{At}$* .

White Rose Research Online URL for this paper:

<https://eprints.whiterose.ac.uk/75078/>

Version: Published Version

---

**Article:**

Andreyev, A. N. [orcid.org/0000-0003-2828-0262](https://orcid.org/0000-0003-2828-0262), Antalic, S., Ackermann, D. et al. (18 more authors) (2013)  *$\beta$ -delayed fission of  $^{192,194}\text{At}$* . Physical Review C. 014317. ISSN 2469-9993

<https://doi.org/10.1103/PhysRevC.87.014317>

---

**Reuse**

Items deposited in White Rose Research Online are protected by copyright, with all rights reserved unless indicated otherwise. They may be downloaded and/or printed for private study, or other acts as permitted by national copyright laws. The publisher or other rights holders may allow further reproduction and re-use of the full text version. This is indicated by the licence information on the White Rose Research Online record for the item.

**Takedown**

If you consider content in White Rose Research Online to be in breach of UK law, please notify us by emailing [eprints@whiterose.ac.uk](mailto:eprints@whiterose.ac.uk) including the URL of the record and the reason for the withdrawal request.

**$\beta$ -delayed fission of  $^{192,194}\text{At}$** 

A. N. Andreyev,<sup>1,2,3,4,11</sup> S. Antalic,<sup>5</sup> D. Ackermann,<sup>6</sup> L. Bianco,<sup>7</sup> S. Franchoo,<sup>8</sup> S. Heinz,<sup>6</sup> F. P. Heßberger,<sup>6,9</sup> S. Hofmann,<sup>6,10</sup> M. Huyse,<sup>1</sup> Z. Kalaninová,<sup>5</sup> I. Kojouharov,<sup>6</sup> B. Kindler,<sup>6</sup> B. Lommel,<sup>6</sup> R. Mann,<sup>6</sup> K. Nishio,<sup>11</sup> R. D. Page,<sup>7</sup> J. J. Ressler,<sup>3</sup> B. Streicher,<sup>5</sup> S. Saro,<sup>5</sup> B. Sulignano,<sup>6</sup> and P. Van Duppen<sup>1</sup>

<sup>1</sup>*Instituut voor Kern- en Stralingsfysica, KU Leuven, University of Leuven, B-3001 Leuven, Belgium*

<sup>2</sup>*School of Engineering and Science, University of the West of Scotland, Paisley PA1 2BE, United Kingdom*

<sup>3</sup>*Department of Chemistry, Simon Fraser University, Burnaby, British Columbia V5A-1S6, Canada*

<sup>4</sup>*TRIUMF, 4004 Wesbrook Mall, Vancouver, British Columbia V6T 2A3, Canada*

<sup>5</sup>*Department of Nuclear Physics and Biophysics, Comenius University, 84248 Bratislava, Slovakia*

<sup>6</sup>*GSI Helmholtzzentrum für Schwerionenforschung, Planckstrasse 1, 64291 Darmstadt, Germany*

<sup>7</sup>*Department of Physics, Oliver Lodge Laboratory, University of Liverpool, Liverpool L69 7ZE, United Kingdom*

<sup>8</sup>*IPN Orsay, F-91406 Orsay Cedex, France*

<sup>9</sup>*Helmholtz-Institut Mainz, Johannes Gutenberg-Universität, 55099 Mainz, Germany*

<sup>10</sup>*Institut für Physik, Goethe-Universität Frankfurt, 60438 Frankfurt, Germany*

<sup>11</sup>*Advanced Science Research Center, Japan Atomic Energy Agency, Tokai, Ibaraki 319-1195, Japan*

(Received 24 August 2012; published 16 January 2013)

By using the recoil-fission correlation technique, the exotic process of beta-delayed fission ( $\beta$ DF) was unambiguously identified in the very neutron-deficient nuclei  $^{192,194}\text{At}$  in experiments at the velocity filter SHIP at Gesellschaft für Schwerionenforschung (GSI). The upper limits for the total kinetic energy release in fission of  $^{192,194}\text{Po}$ , being the daughter products of  $^{192,194}\text{At}$  after  $\beta^+/\text{EC}$  decay, were estimated. The possibility of an unusually high  $\beta$ DF probability for  $^{192}\text{At}$  is discussed.

DOI: [10.1103/PhysRevC.87.014317](https://doi.org/10.1103/PhysRevC.87.014317)

PACS number(s): 24.75.+i, 25.85.-w, 27.80.+w

**I. INTRODUCTION**

Beta-delayed fission ( $\beta$ DF), discovered in 1966 [1–3], is a rare two-step nuclear-decay process in which the parent nuclide first undergoes  $\beta$  decay ( $\beta^+/\text{EC}$  or  $\beta^-$ ) populating excited states in the daughter nucleus. If the excitation energy  $E^*$  of these states is comparable to, or even higher than the fission barrier height  $B_f$  of the daughter nuclide, then fission may happen instantaneously in competition with gamma and/or particle emission. The observed half-life behavior of fission events is then determined by the half-life of the feeding  $\beta$ -decaying parent nucleus. An important experimental quantity is the  $\beta$ DF probability, which is defined as the ratio of the number of  $\beta$ DF decays  $N_{\beta\text{DF}}$  to the number of  $\beta$  decay  $N_\beta$  of the parent nuclide:  $P_{\beta\text{DF}} = \frac{N_{\beta\text{DF}}}{N_\beta}$ .

Beta-delayed fission studies are unique and important probes. First of all, they allow the investigation of fission properties (e.g., fission barrier height, kinetic energy, and mass distributions) of nuclei which otherwise are unfissile in their ground state. Secondly, the excitation energy of the fissioning daughter nucleus is relatively low, limited by the  $Q_{\text{EC}}$  value of the parent nucleus. Therefore, such studies provide unique low-energy fission data in which the shell effects are not washed out and may play a very important role. Furthermore, it is currently believed that in the region of extremely neutron-rich nuclei the  $\beta^-$ -delayed fission (along with the neutron-induced and spontaneous fission) is crucial for understanding such phenomena as the  $r$ -process termination and fission re-cycling and for the production of the heaviest elements in the Universe; see, e.g., Ref. [4].

Prior to our studies,  $\beta$ DF was found in a dozen neutron-deficient nuclei in the uranium and trans-uranium regions; see,

e.g., Refs. [3,5,6] and references therein. These nuclei often have a large  $\beta^+/\text{EC}$ -decay branch with *calculated*  $Q_{\text{EC}}$  values in the range of 3–6 MeV and relatively low fission barriers in the range of 3–7 MeV; see, e.g., Table V of Ref. [7]. Typically, quite low  $\beta$ DF probabilities in the range of  $(10^{-4}\text{--}10^{-1})\%$  were measured for most of the nuclei in this region [2,3,5]. We stress that for majority of these nuclei in the uranium region and also for the nuclides in the lead region, discussed in our work, no experimental  $Q_{\text{EC}}$  and deduced  $B_f$  values exist. Therefore, to treat all nuclei on the same footing we use throughout the paper the calculated finite-range droplet model (FRDM) mass values [8] and calculated fission barriers from finite-range liquid drop model (FRLDM) [7]. We use FRDM because it is more accurate for masses than FRLDM; however, FRDM cannot describe fission barriers because some of its expressions are expansions which are not accurate enough for large deformations; see the discussion in Ref. [7]. In the following, we will denote this model as FRDM/FRLDM, but the use of other mass and fission barrier models will not change our main conclusions, as will be explained below.

Based on the phenomenological approach and comparing calculated  $Q_{\text{EC}}$ (Parent) and  $B_f$ (Daughter) values, the occurrence of  $\beta$ DF in the region of the very neutron-deficient lead isotopes is also expected. First experiments in the lead region were performed by Lazarev *et al.* [9,10] by using complete-fusion reactions induced by heavy ions, and three  $\beta$ DF candidates were identified:  $^{180}\text{Tl}$ ,  $^{188}\text{Bi}$ , and  $^{196}\text{At}$ . Due to the use of mica detectors and a relatively simple production and identification method, only the fact of fission itself and the half-life value of the fissioning candidate nucleus could be deduced in these experiments. To limit the  $A$  and  $Z$  of the most probable parent nucleus, a large series of

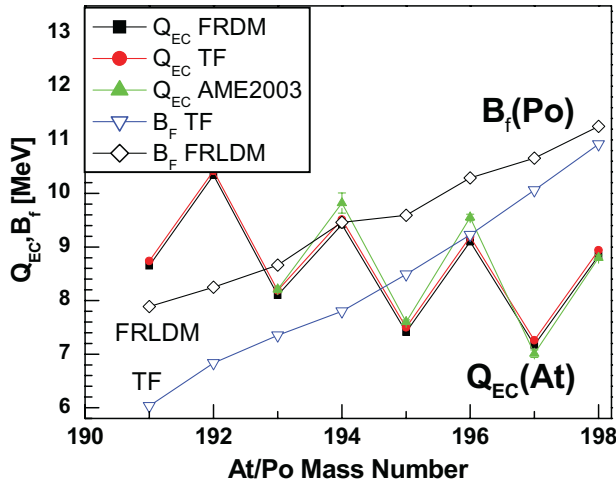


FIG. 1. (Color online) Calculated  $Q_{EC}(At)$  (closed symbols) and  $B_f(Po)$  (open symbols) values according to the FRDM/FRLDM model [7,8] and to the TF model [17]. The experimental or extrapolated  $Q_{EC}$  values, taken from AME2003 [18], are shown by green triangles with uncertainties; see text.

cross-bombardments with different projectile-target combinations had to be performed. For  $\beta DF$  of  $^{180}Tl$ , an unexpectedly low value of  $P_{\beta DF}(^{180}Tl) = 3 \times 10^{-(5 \pm 1)\%}$  [10] was reported, which was lower by a factor of 100 relative to the expectations based on the known systematics in the uranium region [5]. However, in our recent, much more sensitive  $\beta DF$  study of  $^{180}Tl$  [11,12] at the mass-separator ISOLDE, a value of  $P_{\beta DF}(^{180}Tl) = 3.2(2) \times 10^{-3}\%$  was obtained, and the reason for the lower value in the study [9,10] was identified. In the same experiments, the  $\beta DF$  of  $^{178}Tl$  was also observed for the first time [13]. Furthermore, in our recent study at the velocity filter SHIP at Gesellschaft für Schwerionenforschung (GSI),  $\beta DF$  of  $^{186}Bi$  was identified and  $\beta DF$  of  $^{188}Bi$  was unambiguously confirmed [14]. Taken together, both earlier Dubna data and our recent studies firmly establish the phenomenon of  $\beta DF$  in the lead region.

For  $^{196}At$ , which is of a particular interest for the present study, only a half-life estimate of  $0.23^{+0.05}_{-0.03}$  s was deduced in the Dubna study [9,10], which is close to the recent more precise value of  $T_{1/2}(^{196}At) = 0.388(7)$  s [15]. No information on the  $\beta DF$  probability was reported for this nucleus in Ref. [10], but based on the measured fission cross section for  $^{196}At$  from Ref. [10], a value of  $P_{\beta DF}(^{196}At) = 8.8 \times 10^{-2}\%$  with an uncertainty of factor 4 was estimated in Ref. [16].

Figure 1 shows the comparison of the calculated  $Q_{EC}(At)$  and  $B_f(Po)$  values from two different mass models: the FRDM/FRLDM of Refs. [7,8] and the Thomas-Fermi (TF) model of Ref. [17]. The extrapolated or experimental  $Q_{EC}(At)$  values (where available) from AME2003 [18] are also provided for comparison. However, the latter values should be considered with caution since in most of the lightest astatine isotopes there are more than one long-lived nuclear states with often complex and incomplete decay schemes and unknown relative excitation energy. Furthermore, it is not always known which of them is the ground state and for which of them the experimental mass determination was performed or quoted.

A few important features are evident in Fig. 1. First of all, it shows a good agreement for the  $Q_{EC}(At)$  values between the two mass models on the one hand and also between the mass models and experimental data on the other hand. One possible reason for the good agreement between the models is that the  $Q_{EC}$  values are deduced as a difference of the calculated parent and daughter masses. Therefore, even if the two models might give quite different masses, systematically shifted by some value, this shift will largely cancel out in their difference.

Note that, due to the odd-even staggering effect in masses, the  $Q_{EC}$  values of the odd-odd (thus, even- $A$ ) parent astatine isotopes are on average  $\sim 1.5$ – $2$  MeV higher than of their odd- $A$  neighbors. This is one of the reasons why so far all observed  $\beta DF$  nuclides in the uranium and lead regions are odd-odd. Another reason for this, which also applies to  $\beta DF$  of astatine isotopes, is that after  $\beta$  decay of an odd-odd isotope, an even-even daughter is produced, which is expected to fission easier than an odd- $A$  neighbor, produced after the  $\beta$  decay of an odd- $A$  parent nucleus. The very strong (several orders of magnitude) hindrance for spontaneous fission of the odd- $A$  and odd-odd nuclei in comparison with the even-even nuclides is a well established experimental fact—see, e.g., Fig. 3 of Ref. [19]—and is due to the so-called specialization energy arising from the conservation of spin and parity of the odd nucleons in fission. As the maximum excitation energy of the fissioning daughter nucleus in the  $\beta DF$  process is relatively low, similar fission hindrance factors could be also expected for  $\beta DF$ .

Another important feature of Fig. 1 is that both models predict a fast decrease of the calculated fission barriers, from  $\sim 11$  MeV in  $^{198}Po$  to  $\sim 7$ – $8$  MeV in  $^{192}Po$  [7,17], though the rate of decrease is different in the two models discussed. Based on the FRDM/FRLDM values from Fig. 1, the neutron-deficient isotopes  $^{194}At$  ( $Q_{EC} - B_f = -0.04$  MeV) and  $^{192}At$  ( $Q_{EC} - B_f = +2.08$  MeV) should also decay by  $\beta DF$ , with possibly higher  $\beta DF$  branches than  $^{196}At$  ( $Q_{EC} - B_f = -1.19$  MeV). Though somewhat larger  $Q_{EC} - B_f$  values would be obtained for the TF model, this will not change the qualitative expectations on the occurrence of  $\beta DF$  in the lightest astatine nuclides. Namely, the fission of  $^{196}Po$  (the daughter of  $^{196}At$  after  $\beta$  decay), should always be sub-barrier in both models and thus fully defined by the energy-dependent tunneling through the fission barrier. This should be different in the case of fission of  $^{192}Po$ , produced after  $\beta$  decay of the parent  $^{192}At$ , for which one of the largest and positive  $Q_{EC} - B_f = +2.08$  MeV values among all known  $\beta DF$  nuclei is expected; see Table V of Ref. [7] for comparison to all other known cases. Even higher, by  $\sim 1.5$  MeV,  $Q_{EC} - B_f$  values are expected for  $^{192,194}At$  within the TF model; see Fig. 1. In any case, positive  $Q_{EC} - B_f$  values opens up the possibility of feeding states well above the fission barrier, whereby the  $\beta$ -strength function  $S_\beta$  of the parent nucleus, which determines the population pattern of the states in the fissioning daughter product, might become even more crucial for the  $\beta DF$  of  $^{192}At$ . A detailed discussion of the importance of the  $\beta$ -strength function in respect of  $\beta DF$  properties can be found in, e.g., Ref. [20] and references therein.

In this respect,  $\beta DF$  studies provide an alternative (though, admittedly, model-dependent) way of determining the fission

barrier height from the experimentally-determined probability for  $\beta$ -delayed fission; see, e.g., Refs. [16,20–22]. This will help to check the validity of different fission models in very neutron-deficient nuclei, which is one of the goals of our work.

Finally, we mention that one of the important results of our  $\beta$ DF studies of  $^{178,180}\text{Tl}$  at ISOLDE (CERN) [11–13] was the observation of an asymmetric fission fragments mass distribution of their respective daughter (after  $\beta$  decay) products  $^{178,180}\text{Hg}$ . This established a new area of asymmetric fission in low-energy fission in the very neutron-deficient lead region of the nuclidic chart with a neutron-to-proton ratio of  $N/Z \sim 1.22\text{--}1.25$ , in addition to the previously known region in the heavy actinides having the typical values of  $N/Z \sim 1.55\text{--}1.60$ . On the other hand, the low-energy fission experiments ( $E^* \sim 11$  MeV) using electromagnetically induced fission of relativistic radioactive beams at FRS (GSI) [23] identified a broad region of symmetric fission in the light Rn to Th isotopes and, e.g., the fission of  $^{204}\text{Rn}$  ( $N/Z = 1.37$ ) was shown to be symmetric. Therefore, one expects that a transition between the fission asymmetry of  $^{178,180}\text{Hg}$  to the fission symmetry of  $^{204}\text{Rn}$  should happen in between, with the isotopes  $^{192,194,196}\text{Po}$  ( $N/Z \sim 1.29\text{--}1.33$ ) lying exactly along the line connecting the above mentioned mercury and radon isotopes.

The above arguments provided a strong motivation for the present study, which reports on the first unambiguous identification of the  $\beta$ DF process in the neutron-deficient isotopes  $^{192,194}\text{At}$ .

## II. EXPERIMENTAL SETUP AND RESULTS

Two experiments have been performed at the velocity filter SHIP [24,25] at GSI (Darmstadt, Germany). Pulsed beams (5 ms “beam on”/15 ms “beam off”) of  $^{56}\text{Fe}$  and  $^{51}\text{V}$  ions with a typical intensity of 400–600 p nA (1 p nA =  $6.24 \times 10^9$  particles/s) were provided by the UNILAC heavy ion accelerator. Detailed descriptions of both experiments were presented in our papers, which dealt solely with the  $\alpha$ -decay studies of  $^{194}\text{At}$  [26] and of the new isotope  $^{192}\text{At}$  [27]. As the present work concentrates on the  $\beta$ DF data from the same experiments, only the most pertinent experimental details will be provided here.

The isotope  $^{192}\text{At}$  was produced in the complete-fusion reaction  $^{144}\text{Sm}(^{51}\text{V},3n)^{192}\text{At}$ . The targets were prepared by evaporating  $^{144}\text{SmF}_3$  material (96.47% isotopic enrichment) onto a carbon backing of  $40 \mu\text{g}/\text{cm}^2$  thickness and covered with a  $10 \mu\text{g}/\text{cm}^2$  carbon layer to increase the radiative cooling and reduce the sputtering of the material. For  $^{194}\text{At}$ , the  $^{141}\text{Pr}(^{56}\text{Fe},3n)^{194}\text{At}$  reaction was used, with the  $^{141}\text{PrF}_3$  target of 100% natural abundance. In both cases, eight  $\sim 400 \mu\text{g}/\text{cm}^2$  thick targets were mounted on a target wheel, rotating synchronously with the UNILAC macro-pulsing. Data were taken at several beam energies, covering the energy range of the  $2n\text{--}4n$  evaporation channels.

The evaporation residues (recoils), after separation by SHIP were passing through three time-of-flight (ToF) detectors and were implanted into a position-sensitive silicon detector (PSSD), where their subsequent  $\alpha$  and fission decays were

measured. Mylar foils with a typical thickness in the range of 3–4  $\mu\text{m}$  were used in front of the PSSD. Since  $\alpha$  emission is a dominant mode of decay of most of the nuclei produced in both reactions, the identification of nuclides was based on the observation of genetically correlated  $\alpha$ -decay chains along with the excitation function measurements; see Refs. [26,27]. A large-volume four-crystal clover germanium detector was installed behind the PSSD to measure the energies of  $\gamma$  rays detected within 5  $\mu\text{s}$  of the detection of any particle or fission decay in the PSSD. Its performance and  $\gamma$ -ray efficiency for experiments at SHIP were described in Ref. [28].

Upstream of the PSSD, six silicon detectors having the same dimensions (called further “BOX detectors”) were mounted in an open box geometry; see details in Ref. [29]. They were used to measure the energies of  $\alpha$  particles and fission fragments escaping from the PSSD in the backward direction, the latter providing the unique selection of fission fragments; see below.

The energy calibration of the PSSD and of the BOX detectors in the region of fission fragments with energies of up to  $\sim 150$  MeV (see below) relied on the extrapolation of the calibration based on  $\alpha$  decays of bismuth–astatine isotopes (energy range of  $\sim 5\text{--}7.5$  MeV), produced in the same reaction. To account for the pulse height defect and other effects relevant for registration of fission fragments in a silicon detector, a dedicated procedure described in Refs. [30,31] was applied.

### A. $\beta$ DF of $^{194}\text{At}$

Figure 2(a) shows the total energy spectrum of all events registered in the PSSD in the reaction  $^{141}\text{Pr}(^{56}\text{Fe},3n)^{194}\text{At}$  at the beam energy of  $E(^{56}\text{Fe}) = 259(1)$  MeV in front of the target, corresponding to 255 MeV in the middle of the target. A few groups of events can be distinguished in the spectrum. The highest energy group ( $E_{\text{PSSD}} \sim 220\text{--}240$  MeV) corresponds to

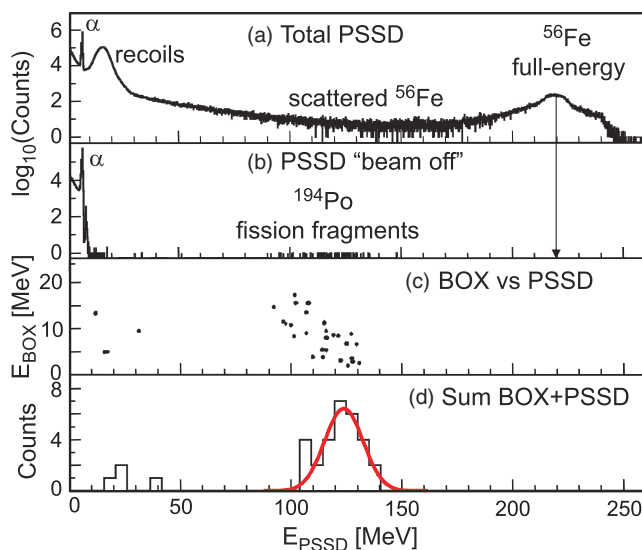


FIG. 2. (Color online) (a) Total energy spectrum in the PSSD in the reaction  $^{141}\text{Pr}(^{56}\text{Fe},3n)^{194}\text{At}$ . (b) The same as (a), but within 15 ms of the “beam off” interval. (c) Two-dimensional BOX vs PSSD spectrum. (d) Sum energy spectrum BOX + PSSD. A Gaussian fit is shown by the red solid line.

the “full” energy  $^{56}\text{Fe}$  beam projectiles “leaking” through the SHIP with a low intensity ( $<0.4$  Hz). The observed energy of this peak is lower than the initial beam energy due to the energy losses in the target, in the carbon foils of the ToF detectors, and in the mylar foil in front of the PSSD, and also due to the pulse-height defect in the PSSD. The large peak at  $\sim 15$  MeV corresponds to the recoils produced in the reaction in the  $xn$ ,  $pxn$ , and  $\alpha xn$  evaporation channels. The broadly distributed structure with the energy in the range of  $\sim 20$ – $200$  MeV includes both lower-energy scattered  $^{56}\text{Fe}$  ions and target-like transfer products. The  $\alpha$  decays of the implanted recoil nuclei and their daughters are seen at  $E_{\text{PSSD}} < 8$  MeV. The zoomed-in  $\alpha$ -decay spectrum for  $^{194}\text{At}$  was given in Ref. [26]. For the sake of the present discussion it is sufficient to mention that we identified two alpha-decaying nuclear states in this nucleus. Presently, their  $\beta$ -branching ratios and relative excitation energy are not known. Following Ref. [26], the two states are denoted further in the text as  $^{194}\text{At}^{m1}$  and  $^{194}\text{At}^{m2}$ , with half-lives of  $T_{1/2}(^{194}\text{At}^{m1}) = 286(7)$  ms and  $T_{1/2}(^{194}\text{At}^{m2}) = 323(7)$  ms. The production cross sections of both isomers were very similar.

Figure 2(b) shows the same spectrum as Fig. 2(a), but registered only during the 15 ms “beam off” time interval, thus only *decay* events can be present in the spectrum. This is indeed proven by the fact that, e.g., the full energy  $^{56}\text{Fe}$  peak and the recoil peak completely disappear from the spectrum.

That is why the 66 high-energy events with the energy of  $\sim 90$ – $150$  MeV in Fig. 2(b) were assigned to fission fragments from the daughter nucleus  $^{194}\text{Po}$  resulting after  $\beta^+ / EC$  decay of  $^{194}\text{At}$ . This conclusion is based on a number of arguments. First of all, a half-life value of  $T_{1/2}(\text{fis}) = 278^{+58}_{-41}$  ms was deduced for these events from the recoil-fission correlation analysis, by searching for correlations between the recoil implantation and its subsequent fission decay in the same position of the PSSD, within a position window of 1 mm. The measured half-life value is in agreement with the half-lives of both  $\alpha$ -decaying isomers in  $^{194}\text{At}$ . Second, 29 of the fission events are double-fold events, in which prompt coincident signals have been measured in the PSSD and in the backward Si BOX detectors; see Fig. 2(c). These events were further used for the estimation of the total kinetic energy (TKE) as discussed below. Third, 41 out of 66 fission events were observed in coincidence with at least one  $\gamma$  decay registered in the Ge detector, which is expected for fission fragments due to their high  $\gamma$ -ray multiplicity. Fission events with  $\gamma$ -ray multiplicity up to 3 were observed by using the four-crystal germanium clover detector. This, however, may also include scattering of  $\gamma$  rays between the crystals. By summing the  $\gamma$ -ray energies from the different crystals, a total  $\gamma$ -ray energy deposition in the clover detector of up to  $\sim 3$  MeV was deduced. Finally, within the limited statistics, the excitation function for fission events has the same shape and beam-energy dependence as the excitation function for  $^{194}\text{At}$  deduced from  $\alpha$  decays; see Fig. 3.

We now turn to the description of the procedure used to estimate the total kinetic energy (TKE) for  $^{194}\text{Po}$ . Due to the recoil implantation in the PSSD at a depth of a few  $\mu\text{m}$ , the initial energies of the individual fission fragments are strongly influenced by energy summing in the PSSD, when one of the

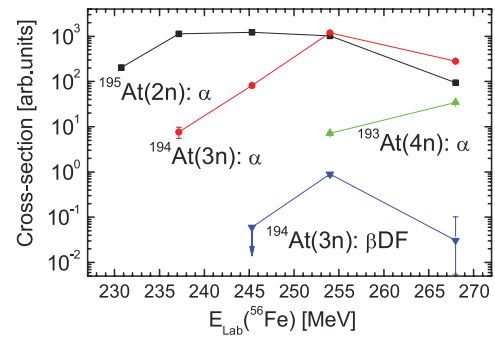


FIG. 3. (Color online) Relative excitation functions for the  $2n$ – $4n$  evaporation channels of the  $^{56}\text{Fe} + ^{141}\text{Pr} \rightarrow ^{197}\text{At}^*$  reaction, deduced from the measured  $\alpha$ -decay rates. For  $^{194}\text{At}$ , the values were summed over two isomers. The excitation function deduced for  $\beta\text{DF}$  events of  $^{194}\text{At}$  is also shown.

fission fragments escapes from the detector in the backward hemisphere thus releasing part of its energy in the PSSD. Consequently, if the escaping coincident fragment is further registered in the BOX detector, its energy is reduced, also due to the necessity to penetrate the dead layers of the PSSD and BOX detectors. Both effects are clearly seen in Fig. 2(c), which gives the two-dimensional spectrum of the energy deposition in the BOX detectors versus the energy deposition in the PSSD registered for events from Fig. 2(b). Indeed, the energy deposition in the BOX detectors is in the range of 2–15 MeV only, which should be compared to the energy deposition of 90–150 MeV in the PSSD.

Furthermore, the pulse height defect (PHD) in the PSSD and BOX detectors for strongly ionizing fission fragments also influences (reduces) their initial energy signal. Only in very rare cases, when the fission happens nearly “horizontal” to the PSSD surface, will both fission fragments be measured in the detector, which would provide a measurement of the total kinetic energy of this fission event, provided a correction for the pulse height defect is applied [30,31]. For example, the event with the highest observed energy of  $\sim 150$  MeV in Fig. 2(b) could be such an event. All above-mentioned effects prohibit us to deduce the initial *individual* fission fragment energies and thus the mass distribution, but we are able to estimate the TKE for fission of  $^{194}\text{Po}$ . The procedure relies on the knowledge of the recoil implantation depth in the PSSD, which can be reliably estimated with the SRIM code [32] based on the reaction kinematics and by accounting for all recoil energy losses starting from the target and finishing with the implantation in the PSSD. Furthermore, the pulse height defect and the influence of the dead layers, for the case of spontaneous fission of  $^{252}\text{No}$  studied at SHIP in previous experiments, are used; see details in Refs. [30,31].

In our case, by summing up the measured energies of 29 coincident fission fragments in the PSSD and BOX detectors, an “apparent”  $\text{TKE}(^{194}\text{Po}) = 124(2)$  MeV with a full width at half magnitude (FWHM) value of 21 MeV was obtained, derived from the Gaussian fit of the obtained sum spectrum; see Fig. 2(d). This value was further corrected by 36(7) MeV due to the pulse height defect and dead layers according to the procedure described above and in Refs. [30,31], which

resulted in the “unperturbed” total kinetic energy release of  $\text{TKE}(^{194}\text{Po}) = 160(8)$  MeV. This value would be in agreement, within the quoted uncertainty, with the value of  $\sim 153$  MeV expected according to the so-called Viola systematics [33].

However, we stress that the above procedure from Refs. [30,31] relies on the use of the fission data and correction procedure for the well studied spontaneous fission of a much heavier nucleus,  $^{252}\text{No}$ , with the tabulated TKE value of  $\sim 195$  MeV. In this case, the most probable light and heavy fission fragments have masses in the vicinity of  $M_L \sim 110$  and  $M_H \sim 142$ , with a typical neutron-to-proton ratio of  $N/Z \sim 1.47$ , which is similar to the  $N/Z$  value of the parent nucleus  $^{252}\text{No}$ . All this is very different for the fission of  $^{194}\text{Po}$  ( $N/Z \sim 1.31$ ) with the expected TKE value of  $\sim 153$  MeV [33]. Furthermore, the fission fragments of  $^{194}\text{Po}$  are expected to have both lower atomic numbers and masses, most probably around  $M_{L,H} \sim 80\text{--}100$ , and lower  $N/Z$  values, similar to that for  $^{194}\text{Po}$ . Clearly, both the PHD values and the energy losses in the dead layers of the PSSD and BOX detectors for lighter fission fragments of  $^{194}\text{Po}$  will be different relative to those for the much heavier fission fragments of the reference nucleus  $^{252}\text{No}$ . Therefore, as a detailed account of these effects is not possible based on our dataset, we prefer to treat the above-deduced TKE value for  $^{194}\text{Po}$  as the *upper limit* only.

The total production cross section of  $^{194}\text{At}$  at the maximum of the excitation function was deduced as  $1.3(4) \mu\text{b}$  [26], with an approximately equal relative population of two isomeric states. The ratio of numbers of  $\beta\text{DF}$  to  $\alpha$  decays for  $^{194}\text{At}$ , corrected for the respective detection efficiencies in the PSSD, is  $\frac{N_{\beta\text{DF}}}{N_{\alpha}} = 6.5(8) \times 10^{-4}$ . The measured  $\beta\text{DF}$  rate of  $^{194}\text{At}$  was  $\sim 4$  fissions per hour at the maximum of the excitation function for the  $3n$  channel. Due to the presence of two isomers with similar half-life in  $^{194}\text{At}$ , we cannot disentangle which of them (or both?) decays via  $\beta\text{DF}$ . Furthermore, presently, no experimentally measured  $\beta$ -branching ratios are known for the two isomers, while these values are necessary for the determination of their  $\beta\text{DF}$  probability. Due to above reasons, no experimental  $\beta\text{DF}$  probability for  $^{194}\text{At}$  can be deduced from the present data. However, in the Discussion section, an attempt to provide a qualitative estimate for  $P_{\beta\text{DF}}(^{192,194}\text{At})$  will be presented.

For completeness, we mention that 16 fission events in the PSSD “beam off” energy spectrum were also observed as a byproduct of another experiment at SHIP in which the new isotope  $^{194}\text{Rn}$  [ $T_{1/2} = 0.78(16)$  ms] was identified in the  $^{144}\text{Sm}(^{52}\text{Cr}, 2n)^{194}\text{Rn}$  reaction [34]. The half-life value of  $T_{1/2} = 362_{-74}^{+124}$  ms was deduced for these fission events, which confirms the identification of  $\beta\text{DF}$  fission of the  $^{194}\text{At}$  isotope, which was produced much more abundantly in the  $^{144}\text{Sm}(^{52}\text{Cr}, pn)^{194}\text{At}$  reaction channel in comparison with  $^{194}\text{Rn}$ . In agreement with the above-mentioned data for the  $^{56}\text{Fe}$ -induced reaction, a similar ratio of  $\frac{N_{\beta\text{DF}}}{N_{\alpha}} = 5.4(14) \times 10^{-4}$  was deduced for the numbers of  $\beta\text{DF}$  and  $\alpha$  decays of  $^{194}\text{At}$  in this reaction, corrected for the respective registration efficiencies. The  $\beta\text{DF}$  rate in this reaction was  $\sim 0.25$  fissions per hour. The much lower fission rate in this reaction, in comparison with the  $3n$  channel of the  $^{141}\text{Pr}(^{56}\text{Fe}, 3n)^{194}\text{At}$

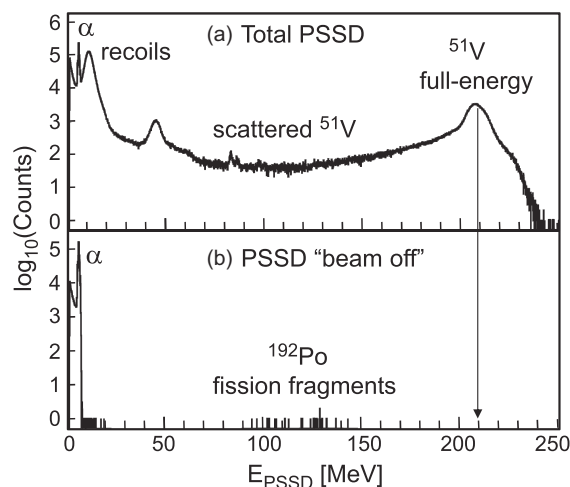


FIG. 4. (a) Total energy spectrum in the PSSD for the reaction  $^{144}\text{Sm}(^{51}\text{V}, 3n)^{192}\text{At}$ . (b) The same as (a), but within 15 ms of the “beam off” interval; see text for details.

reaction, is explained by the fact that the  $pn$  channel of  $^{52}\text{Cr}$ -induced reaction was slightly sub-barrier.

### B. $\beta\text{DF}$ of $^{192}\text{At}$

By using the same method, the  $\beta\text{DF}$  of  $^{192}\text{At}$  was identified in the  $^{144}\text{Sm}(^{51}\text{V}, 3n)^{192}\text{At}$  reaction at a beam energy of  $E(^{51}\text{V}) = 230(1)$  MeV in middle of the target. Figure 4(a) shows the total PSSD energy spectrum, measured for this reaction, with all the peaks similar to those in Fig. 2(a). The zoomed-in  $\alpha$ -decay spectrum in the region of 7–8 MeV was shown and discussed in our study [27]. In Fig. 4(b) only decay events occurred in the “beam off” interval are shown. In total 24 fission events in the energy range of  $\sim 90\text{--}150$  MeV have been observed during the “beam of” interval and attributed to the fission of the daughter isotope  $^{192}\text{Po}$ , resulting after  $\beta^+/\text{EC}$  decay of the parent  $^{192}\text{At}$  nucleus. Similarly to  $^{194}\text{At}$ , most of these fission events were observed in coincidence with  $\gamma$  rays, up to a  $\gamma$ -ray multiplicity of 3 and the maximum total energy deposition in the Ge detector of  $\sim 1.8$  MeV.

Eleven out of total 24 fission events were double-fold PSSD-BOX coincident events. By using the same procedure as for  $^{194}\text{Po}$ , an *upper limit* for the total kinetic energy release  $\text{TKE}(^{192}\text{Po}) = 169(10)$  MeV was deduced for these PSSD-BOX coincident events. This value is quite higher than the value of  $\sim 153$  MeV expected for  $^{192}\text{Po}$  based on the Viola systematics [33]. As in the case of  $^{194}\text{Po}$ , this could be due to the use of  $^{252}\text{No}$  as a reference nucleus.

Based on the recoil-fission correlation analysis within the time interval of 800 ms, a good preceding recoil implantation was found for 23 out of 24 fission events in Fig. 4(b). Figure 5 shows the time distribution  $\Delta t(\text{Recoil-fission})$  for these 23 fission events, based on which the half-life value of  $T_{1/2} = 110_{-18}^{+26}$  ms was deduced, which is consistent with a value of  $T_{1/2} = 88(6)$  ms for the  $(9^-, 10^-)$  isomer in  $^{192}\text{At}$  [27]. We note that five fission events had the recoil-fission time difference of less than 20 ms, thus some of them could still be attributed to the  $\beta\text{DF}$  decay of the 11-ms isomer of  $^{192}\text{At}$ . However, based on

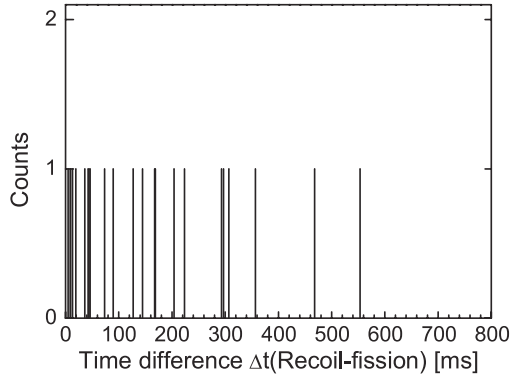


FIG. 5. Time distribution  $\Delta t(\text{Recoil-fission})$  for  $^{192}\text{At}$  deduced from the recoil-fission correlation analysis for 23 fission events from Fig. 4(b).

the exponential decay law, most of these events could also be accounted as due to the decay of the 88-ms isomer. Therefore, although our analysis tentatively indicates that most probably only the 88-ms isomer of  $^{192}\text{At}$  undergoes  $\beta\text{DF}$ , we prefer not to draw an unambiguous conclusion whether both isomers or only the longer-lived isomer of  $^{192}\text{At}$  undergo  $\beta\text{DF}$ . Taken together with the unknown  $\beta$ -branching ratios for both isomers in  $^{192}\text{At}$ , this prohibits us from deducing the experimental  $\beta\text{DF}$  probabilities for these isomers. However, similar to  $^{194}\text{At}$  case, in the Discussion section we make an attempt of a qualitative estimate of  $\beta\text{DF}$  probability for  $^{192}\text{At}$ .

The total production cross section of  $^{192}\text{At}$  at the maximum of the excitation function was deduced as 40(10) nb in Ref. [27], with the relative population ratio of two isomeric states of  $\frac{I(^{192}\text{At}, 88 \text{ ms})}{I(^{192}\text{At}, 11 \text{ ms})} \sim 1.4$ , as deduced from their  $\alpha$ -decay intensities. A ratio of  $\frac{N_{\beta\text{DF}}}{N_{\alpha}} = 4.2(9) \times 10^{-3}$  was deduced for the numbers of  $\beta\text{DF}$  and all  $\alpha$  decays of  $^{192}\text{At}$ , corrected for respective registration efficiencies, which is 6.5(16) times larger than in the case of  $^{194}\text{At}$ . This important fact will be discussed in the next section. The measured  $\beta\text{DF}$  rate of  $^{192}\text{At}$  was  $\sim 0.4$  fissions per hour at the maximum of the excitation function for the  $3n$  channel.

### III. DISCUSSION

#### A. Upper limits for the total kinetic energy for $^{192,194}\text{Po}$

Figure 6 compares the deduced upper limits for the total kinetic energy values for  $^{192,194}\text{Po}$  with the known data in the heavier nuclei and also with the Viola fit [33], shown by the black solid line. First of all, we point out that, if the fission mechanisms of  $^{192,194}\text{Po}$  were similar, very similar TKE values would be expected. A recent example for this is provided by, e.g., our data for the TKE values of  $^{178,180}\text{Hg}$ , which are very similar to each other; see Ref. [13]. Therefore, the observed TKE difference (though still within the experimental uncertainties) between  $^{192,194}\text{Po}$  might indicate a difference in their fission mechanism. However, most probably, this difference is just due to the deficiencies of our experimental procedure used to deduce the TKE values; see the discussion in the previous sections.

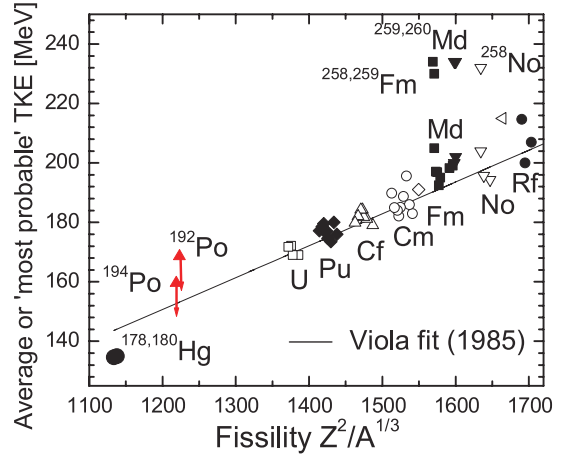


FIG. 6. (Color online) Total kinetic energy (TKE) values as a function of the fissility parameter  $Z^2/A^{1/3}$ ; data are taken from [35]. Our upper limits for TKEs of  $^{192,194}\text{Po}$  are shown by triangles with downward arrows; the data for  $^{178,180}\text{Hg}$  (nearly indistinguishable on this scale) are from Refs. [12,13]. The Viola fit [33] is shown by the solid line; see the text.

Similarly, the fact that the deduced upper limits lie by  $\sim 8\text{--}15$  MeV higher than one would expect based on the Viola systematics, (but still within a 1–2 sigma limit relative to it) should most probably be attributed to the experimental procedure used.

#### B. A qualitative estimate of the $\beta\text{DF}$ probabilities for $^{192,194}\text{At}$

As discussed earlier, due to the lack of a detailed decay scheme and  $\beta$ -decay branching ratios of both isomers in  $^{192,194}\text{At}$ , their experimental  $\beta\text{DF}$  probabilities cannot be deduced from our data. However, an estimate is still possible, and below we will first start with a very general estimate, which does not require knowledge of the relevant branching ratios. The goal of such an exercise is to show the possible magnitudes and trends of the  $P_{\beta\text{DF}}$  values by moving to the most neutron-deficient astatine isotopes. This estimate will be then followed by a more quantitative derivation.

To start, we compare the deduced ratios of the numbers of  $\beta\text{DF}$  and  $\alpha$  decays for  $^{194}\text{At}$  ( $\frac{N_{\beta\text{DF}}}{N_{\alpha}} = 6.5(8) \times 10^{-4}$ ) and for  $^{192}\text{At}$  ( $\frac{N_{\beta\text{DF}}}{N_{\alpha}} = 4.2(9) \times 10^{-3}$ ). As both  $^{194}\text{At}$  and  $^{192}\text{At}$  are expected to have  $\alpha$ -branching ratios over 90% (see below), the number of detected  $\alpha$  decays, corrected for the PSSD detection efficiency, is a good measure of the total number of astatine nuclei,  $N_{\alpha}$ , implanted in the PSSD. Therefore, based on the definition of the  $\beta\text{DF}$  probability, one can write, e.g.,  $P_{\beta\text{DF}}(^{194}\text{At}) = \frac{N_{\beta\text{DF}}(^{194}\text{At})}{N_{\beta}(^{194}\text{At})} \sim \frac{N_{\beta\text{DF}}(^{194}\text{At})}{N_{\alpha}(^{194}\text{At}) \times b_{\beta}(^{194}\text{At})}$  (the same formula applies for  $^{192}\text{At}$  as well). It can be further safely assumed that the  $\beta$ -branching ratio  $b_{\beta}(^{194}\text{At})$  is larger than that for the more neutron-deficient  $^{192}\text{At}$ , therefore the  $P_{\beta\text{DF}}(^{192}\text{At})$  value is expected to be at least a factor of 6.5(16) larger than that for  $^{194}\text{At}$ .

Now, we will try to deduce more quantitative estimate of  $\beta\text{DF}$  probabilities. In a first step, by comparing the experimental half-life values and calculated partial  $\beta$ -decay

half-lives within the QRPA framework of Ref. [36],  $T_{1/2,\beta}(^{192}\text{At}) = 1.9$  s and  $T_{1/2,\beta}(^{194}\text{At}) = 3.6$  s, the estimates for the  $\beta$ -branching ratios were made for  $^{192,194}\text{At}$ . The model [36] is based on the same FRDM and folded-Yukawa single-particle potential as used to calculate  $Q_{EC}$  values in Fig. 1. Specifically, the following values were obtained for two isomers in  $^{192}\text{At}$ :  $b_{\beta}(^{192}\text{At}, 11 \text{ ms}) \sim 0.6\%$  and  $b_{\beta}(^{192}\text{At}, 88 \text{ ms}) \sim 4.6\%$ . As the half-lives of both isomers in  $^{194}\text{At}$  are quite similar, a single estimate of  $b_{\beta}(^{194}\text{At}, 300 \text{ ms}) \sim 8.3\%$  was derived for both isomers. Comparable values (within a factor of 2) could be obtained for  $^{192}\text{At}$  if one uses the data from Ref. [37], while no calculated data for  $^{194}\text{At}$  were given in this work. Based on the evaluations in the theoretical studies of  $\beta$  decay—see, e.g., Refs. [22,36,37]—the calculated partial  $\beta$ -decay values should be valid within a factor of 2–3 for most cases, which is one of the dominant uncertainties in our estimate below. We also mention that the estimated  $b_{\beta}$  values for  $^{194}\text{At}$  and for the 88-ms isomer of  $^{192}\text{At}$  are in a reasonable agreement with the values expected from the extrapolation of the experimentally known  $\beta$ -branching ratios for the heavier astatine isotopes.

As mentioned earlier, a nearly equal population, as deduced from  $\alpha$ -decay intensities, of two isomeric states in  $^{194}\text{At}$  was deduced in Ref. [26]. Therefore, in the second step, we assumed that only one of the isomers in  $^{194}\text{At}$  undergoes  $\beta$ DF and compared the observed number of 66 fission decays of  $^{194}\text{Po}$  to the number of  $\alpha$  decays from *one* isomer of  $^{194}\text{At}$ , both normalized on the corresponding detection efficiencies. Then, with the use of the calculated branching ratio  $b_{\beta} \sim 8.3\%$ , an estimate of  $P_{\beta\text{DF}}(^{194}\text{At}) \sim 1.6\%$  could be obtained for this isomer. The uncertainty of this value is defined by the uncertainty of the calculated  $\beta$ -branching ratio quoted above and also by the assumption on the specific division of the observed fission events between two isomers. It is evident that if both isomers of  $^{194}\text{At}$  have similar  $\beta$ -branching ratios of  $\sim 8.3\%$  and both undergo  $\beta$ DF with a similar probability, then each of them would have the  $\beta$ DF probability of  $\sim 0.8\%$ . On the other hand, lower (larger)  $\beta$ -branching ratios would result in larger (lower)  $P_{\beta\text{DF}}$  values. In any case, it is clear that the  $\beta$ DF probability for  $^{194}\text{At}$  should be in the percents range, which would be approximately an order of magnitude larger than the value of  $P_{\beta\text{DF}}(^{196}\text{At}) \sim 8.8 \times 10^{-2}\%$  deduced in Ref. [16], albeit with an uncertainty of a factor of 4.

In a similar way, by assuming that all 23 fission events, for which the time distribution could be measured, originate from the 88-ms isomer of  $^{192}\text{At}$  only, and using the calculated branching ratio  $b_{\beta}(^{192}\text{At}, 88 \text{ ms}) = 4.6\%$  and the population intensity relative to the 11-ms isomer, an *estimate* of  $P_{\beta\text{DF}}(^{192}\text{At}, 88 \text{ ms}) \sim 16\%$  could be obtained. As discussed earlier, only a few of the correlated 23 fission events could in principle be attributed to the shorter-lived 11-ms isomer, which will not change considerably the deduced  $\beta$ DF probability for the 88-ms isomer.

It is important to note that if we assume  $P_{\beta\text{DF}}(^{192}\text{At}, 88 \text{ ms}) = 100\%$ , a lower limit of  $b_{\beta} = 0.7\%$  would result for this isomer. In other words, to account for the observed rate of fission events, if all are attributed to the 88-ms isomer, this isomer cannot have a  $\beta$ -branching ratio of less than 0.7%.

Note that by applying the same procedure for the 11-ms isomer, and in the limiting case when one attributes the five fission events with a recoil-fission time difference of less than 20 ms to the shorter-lived isomer, and by accounting for the relative population of the 11-ms isomer, a value of  $P_{\beta\text{DF}}(^{192}\text{At}, 11 \text{ ms}) \sim 35\%$  was obtained. On the other hand, a value  $P_{\beta\text{DF}}(^{192}\text{At}, 11 \text{ ms}) \sim 7\%$  would be obtained in the limiting case when only one fission event was assigned to this isomer.

To conclude this highly qualitative discussion, within the relatively large uncertainty associated with the deduction of the  $P_{\beta\text{DF}}$  estimates for  $^{192,194}\text{At}$ , one observes a definite trend of a strong increase of the respective values from  $^{196}\text{At}$  to  $^{194}\text{At}$  and further to  $^{192}\text{At}$ . Especially in the case of  $^{192}\text{At}$ , some of the largest  $P_{\beta\text{DF}}$  values among all known  $\beta$ DF isotopes could be estimated. This is what one indeed anticipates in view of the one of largest  $Q_{EC} - B_f = +2.08$  MeV values expected for  $\beta$ DF of  $^{192}\text{At}$ . Due to this, the states well above the top of the fission barrier in the fissioning daughter nucleus  $^{192}\text{Po}$  could be populated with the higher probability, which should facilitate fission. The estimated values for  $^{192,194}\text{At}$  are substantially higher than the typical  $\beta$ DF probabilities in the uranium region, which are in the range of  $(10^{-4}-10^{-1})\%$  [5]. To our knowledge, only in the  $\beta$ DF of  $^{246}\text{Md}$  was a similarly high value of  $P_{\beta\text{DF}} \geq 10\%$  recently proposed [6].

#### IV. CONCLUSIONS

The  $\beta$ -delayed fission was unambiguously identified (with  $Z$  and  $A$  determination of the parent fissioning isotope) in the very neutron-deficient nuclides  $^{192,194}\text{At}$ , and the upper limits for the TKE values for the fission of their daughter products (after  $\beta$  decay),  $^{192,194}\text{Po}$ , were estimated for the first time.

As far as the  $\beta$ DF probabilities are concerned, a qualitative analysis for  $^{192,194}\text{At}$  results in some of the largest  $P_{\beta\text{DF}}$  values ever deduced. In particular, for two isomers in  $^{192}\text{At}$ , values in the range of 7%–35% could be estimated, these being the largest ever reported so far for  $\beta$ DF. Experimental measurements of the  $\beta$ -branching ratios and of the  $\beta$ -strength functions for both isomers in  $^{192,194}\text{At}$  are necessary to shed more light on this important question.

The importance of these nuclei is due to the fact that they are lying in the transitional region between  $^{178,180}\text{Hg}$  exhibiting asymmetric low-energy fission and  $^{204}\text{Rn}$  which fissions symmetrically at similar excitation energies [23]. Therefore further dedicated  $\beta$ DF studies with higher statistics are required for  $^{192,194}\text{At}$ , aimed at coincident fission fragment measurements similar to those, performed in our study of  $^{180}\text{Hg}$  at the mass-separator ISOLDE (CERN) [11,12]. In this type of experiments, unperturbed energies of singles and coincident fission fragments can be measured, which uniquely identifies their masses and provides quite precise TKE values; see Ref. [12]. These experiments will also allow  $\gamma$ -ray energy measurements in better conditions, by possibly applying large Ge arrays installed around the Si detectors.

Following the recent successful development of the radioactive astatine beams with the Resonance Ionization Laser Ion Source at ISOLDE [38], systematic dedicated  $\beta$ DF studies



of  $^{194,196}\text{At}$  are now possible and will be performed in the near future. On the other hand, the shorter-lived isotope  $^{192}\text{At}$  might not be yet accessible at ISOL-based facilities and must be studied at recoil separators, possibly followed by “In Gas Laser Ionization and Spectroscopy” (IGLIS) systems [39].

### ACKNOWLEDGMENTS

We thank the UNILAC staff for providing the stable and high intensity  $^{56}\text{Fe}$  and  $^{51}\text{V}$  beams. This work was supported by

FWO-Vlaanderen (Belgium), by GOA/2004/03 (BOF–K.U. Leuven), by the IUAP–Belgian State Belgian Science Policy (BriX network P6/23 and P7/12), by the European Community FP7 Capacities, Contract No. ENSAR 262010, by the UK Science and Technology Facilities Council (STFC), by the Reimei Foundation of Advanced Research Science Center (ASRC, JAEA), by the DAIWA Anglo-Japanese foundation, by the Slovak Research and Development Agency (Contract No. APVV-0105-10), and by the Slovak grant agency VEGA (Noncontract No. 1/0613/11). A.N.A. and J.J.R. were partially supported by the NSERC of Canada.

- 
- [1] V. I. Kuznetsov, N. K. Skobelev, G. N. Flerov, *Yad. Fiz.* **4**, 279 (1966) [*Sov. J. Nucl. Phys.* **4**, 202 (1967)]; *Yad. Fiz.* **5**, 271 (1967) [*Sov. J. Nucl. Phys.* **5**, 191 (1967)].
- [2] V. I. Kuznetsov and N. K. Skobelev, *Phys. Part. Nucl.* **30**, 666 (1999).
- [3] H. L. Hall and D. C. Hoffman, *Annu. Rev. Nucl. Part. Sci.* **42**, 147 (1992).
- [4] I. V. Panov *et al.*, *Nucl. Phys. A* **747**, 633 (2005).
- [5] D. A. Shaughnessy *et al.*, *Phys. Rev. C* **65**, 024612 (2002).
- [6] S. Antalic *et al.*, *Eur. Phys. J. A* **43**, 35 (2010).
- [7] P. Möller, A. J. Sierk, T. Ichikawa, A. Iwamoto, R. Bengtsson, H. Uhrenholt, and S. Aberg, *Phys. Rev. C* **79**, 064304 (2009).
- [8] P. Möller *et al.*, *At. Data Nucl. Data Tables* **59**, 185 (1995).
- [9] Yu. A. Lazarev *et al.*, *Europhys. Lett.* **4**, 893 (1987).
- [10] Yu. A. Lazarev *et al.*, in *Proceedings of the 6th International Conference On Atomic Masses and Fundamental Constants, Bernkastel-Kues*, IOP Conf. Proc. No. N132 (Institute of Physics, London, 1992), p. 739.
- [11] A. N. Andreyev *et al.*, *Phys. Rev. Lett.* **105**, 252502 (2010).
- [12] J. Elseviers *et al.* [*Phys. Rev. C* (to be published)].
- [13] V. Liberati *et al.* (unpublished).
- [14] J. F. W. Lane *et al.*, *Phys. Rev. C* **87**, 014318 (2013).
- [15] M. B. Smith *et al.*, *J. Phys. G* **26**, 787 (2000).
- [16] A. N. Andreyev *et al.*, *Phys. Lett. B* **312**, 49 (1993).
- [17] W. D. Myers and W. J. Swiatecki, *Phys. Rev. C* **60**, 014606 (1999).
- [18] G. Audi, A. H. Wapstra, and C. Thibault, *Nucl. Phys. A* **729**, 337 (2003).
- [19] D. C. Hoffman, *Nucl. Phys.* **502**, 21 (1989).
- [20] M. Veselsky, A. N. Andreyev, S. Antalic, M. Huyse, P. Moller, K. Nishio, A. J. Sierk, P. Van Duppen, and M. Venhart, *Phys. Rev. C* **86**, 024308 (2012).
- [21] D. Habs *et al.*, *Z. Phys. A* **285**, 53 (1978).
- [22] A. Staudt, M. Hirsch, K. Muto, and H. V. Klapdor-Kleingrothaus, *Phys. Rev. Lett.* **65**, 1543 (1990).
- [23] K.-H. Schmidt *et al.*, *Nucl. Phys. A* **693**, 169 (2001); **665**, 221 (2000).
- [24] G. Münzenberg *et al.*, *Nucl. Instrum. Methods* **161**, 65 (1979).
- [25] S. Hofmann and G. Münzenberg, *Rev. Mod. Phys.* **72**, 733 (2000).
- [26] A. N. Andreyev *et al.*, *Phys. Rev. C* **79**, 064320 (2009).
- [27] A. N. Andreyev *et al.*, *Phys. Rev. C* **73**, 024317 (2006).
- [28] F. P. Heßberger *et al.*, *Eur. Phys. J. A* **43**, 55 (2010).
- [29] A. N. Andreyev *et al.*, *Nucl. Instrum. Methods A* **533**, 409 (2004).
- [30] S. Hofmann *et al.*, *Eur. Phys. J. A* **32**, 251 (2007).
- [31] K. Nishio *et al.*, in *Tours Symposium on Nuclear Physics VI*, Tours, France, 2006, edited by M. Arnould, M. Lewitowicz, H. Emling, H. Akimune, M. Ohta, H. Utsunomiya, T. Wada, and T. Yamagata, AIP Conf. Proc. No. 891 (AIP, New York, 2007), p. 71.
- [32] J. F. Ziegler, SRIM code, <http://www.srim.org/SRIM/SRIMLEGL.htm>.
- [33] V. E. Viola, K. Kwiatkowski, and M. Walker, *Phys. Rev. C* **31**, 1550 (1985).
- [34] A. N. Andreyev *et al.*, *Phys. Rev. C* **74**, 064303 (2006).
- [35] D. C. Hoffman and M. R. Lane, *Radiochim. Acta* **70/71**, 135 (1995).
- [36] P. Möller, J. R. Nix, and K.-L. Kratz, *At. Data Nucl. Data Tables* **66**, 131 (1997).
- [37] M. Hirsh *et al.*, *At. Data Nucl. Data Tables* **53**, 165 (1993).
- [38] S. Rothe *et al.*, *Nat. Commun.* (to be published).
- [39] R. Ferrer *et al.*, *Nucl. Instrum. Methods B* **291**, 29 (2012).